Vibrational Fine Structures Revealed by the Frequency-to-Time Fourier Transform of the Transient Spectrum in Bacteriorhodopsin

Atsushi Yabushita*,† and Takayoshi Kobayashi†,‡,§,⊥

Department of Electrophysics, National Chiao-Tung University, 1001 Ta Hsueh Road, Hsinchu 3005, Taiwan, Department of Applied Physics and Chemistry and Institute for Laser Science, The University of Electro-Communications, 1-5-1 Chofugaoka, Chofu, Tokyo, 182-8585, Japan, JST, ICORP, Ultrashort Pulse Laser Project, 4-1-8 Honcho, Kawaguchi, Saitama, Japan, and Institute of Laser Engineering, Osaka University, 2-6 Yamada-Oka, Suita, Osaka 565-0971, Japan

Received: September 17, 2009; Revised Manuscript Received: February 6, 2010

A vibrational progression that is hidden in a featureless spectrum of induced absorption and stimulated emission was found in time-resolved absorption change spectra. The ultrahigh time resolution of the pump−probe measurement made by using an ultrashort laser pulse localizes the wave packet along the potential multimode hyper surfaces, represented by a vibrational progression. The transition energy of the induced absorption and stimulated emission corresponds to a localized point (space) on the hyper surface, which is visited by the wave packets with fixed phases.

1. Introduction

Bacteriorhodopsin (bR) is a photoactive retinoid protein with a proton-pumping function that generates a pH gradient across the cellular membrane, using solar energy to synthesize ATP. This pumping involves a change in a local structure of the protein near the retinal molecule. The conformational change in the protein is initiated by the optically triggered trans−cis photoisomerization, which is closely related to the photoisomerization of retinal from 11-cis to the all-trans configuration in rhodopsin, which is the functional pigment in the visual sensor process.[1] The absorption of a photon by the chromophore molecule in the retinal causes isomerization around the C_{13}═C_{14} double bond followed by photocycle with several intermediates that have distinct spectra. Because of its interesting functionality, bR has been widely studied both theoretically[2,3] and experimentally.[4−10] An ultrafast switch that exploits its ultrafast photoisomerization has also been implemented,[11] although the mechanism remains controversial. Ruhman et al. determined experimentally that locked-retinal that is contained in bR undergoes a similar photoinduced spectral change to that of ordinary bR.[12,13] On the basis of theoretical models of the photoisomerization mechanism, the groups of Olivucci[2,15] and Schulten[3,16] proposed "a two-state, two-mode model" and "a three-state model", respectively.

Ultrafast dynamics of chemical reactions have been studied by using ultrafast spectroscopy, which has demonstrated the transient existence of intermediate species in the reactions.[17,18] Ultrafast spectroscopy is a method that complements the electron diffraction method presented by Miller[19] et al. and Zewail[20] and the X-ray diffraction methods proposed by Anfinrud et al.[21] Instantaneous vibrational amplitude detection with a subfemtosecond resolution, which is demonstrated in this work, provides a much higher time resolution than electron or X-ray diffraction. Additionally, the method can be used to make measurements of amorphous and liquid-phase materials, to which X-ray or electron diffraction cannot easily be applied. In the authors' earlier work,[22] we detected ultrafast changes in the frequencies of in-plane and out-of-plane bending modes caused by a structural change in real time during photoisomerization. Femtosecond stimulated Raman spectroscopy with high time and spectral resolutions was employed to observe time-dependent conformational changes,[23] but the method does not yield information on the vibrational phase, which can be obtained in the pump−probe measurement.

As was discussed in a recent work,[24] time-resolved measurement of absorbance change involves wave packets on both potential surfaces of the electronic ground state and the excited state. Detailed observations made in the authors' recent investigation[25] on the photoexcited dynamics revealed that the primary process of the photoisomerization begins with the activation of the C═N stretching mode of the highest frequency, which decays in 30 fs, followed by that of the C═C stretching mode, which has a slightly lower frequency. The C═C mode is modulated at frequencies of 142 ± 35, 105 ± 3, 158 ± 3, and 150 ± 18 cm^{-1} in wavelength ranges of 505−530 (S), 540−600 (M), 610−630 (L_1), and 635−663 nm (L_2), respectively, corresponding to the excited state (H state), ground state, I intermediate, and J intermediate, respectively. In the first three ranges (S, M, L_1), the lifetimes were <100, 1050 ± 180, and 270 ± 30 fs (with a rise time of 160 ± 20 fs), respectively.

In this work, pump−probe measurements of bR were made by using ultrashort visible laser pulses, to obtain simultaneously ultrafast time-resolved absorbance change (ΔA) spectra at 128 wavelengths. The ΔA spectra revealed a vibrational progression hidden in a featureless spectrum of induced absorption and stimulated emission. This observation can be made because of the localization of the wave packet along the potential multimode hyper surfaces. The transition energy of the induced absorption or stimulated emission corresponds to a localized point (space) on the hyper surface, which is visited by the wave packets with fixed phases.

* To whom correspondence should be addressed. E-mail address: yabushita@mail.nctu.edu.tw.
† National Chiao Tung University.
‡ The University of Electro-Communications.
§ JST.
⊥ Osaka University.

10.1021/jp9090014
Published on Web 03/11/2010

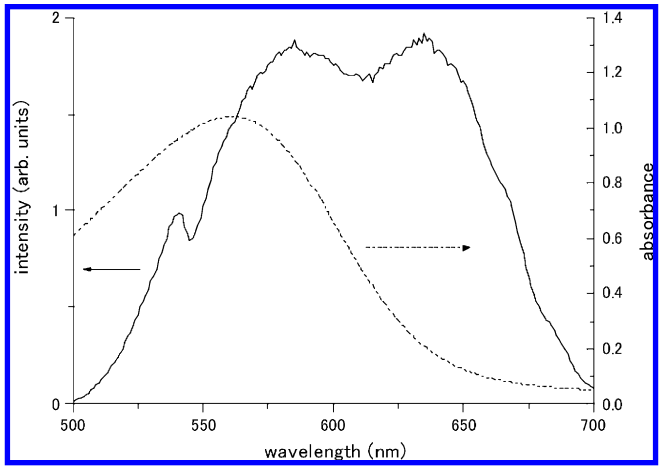

Figure 1. Laser spectrum (solid curve) and absorption spectrum (dashed curve) of bacteriorhodopsin.

2. Experimental Section

A noncollinear optical parametric amplifier (NOPA)[26−28] was adopted as a light source in the pump−probe experiment, as described elsewhere.[29−31] Several key features of the system are briefly described below. The output pulse from the NOPA was compressed by using a compressor that was composed of a pair of prisms and chirp mirrors. The pulse duration was sub-10 fs and the spectral range covered 520 to 750 nm, within which the spectral phase was almost constant, resulting in the Fourier-transform-limited pulses. The pulse energies of the pump and probe were about 10 and 1 nJ, respectively. A 128-channel lock-in amplifier was employed as a phase-sensitive broadband detector. All of the experiments were conducted at room temperature (293 ± 1 K).

3. Results and Discussion

Figure 1 presents the laser spectrum and the absorption spectrum of the bR sample. The absorbed photon distribution spectrum, also displayed in Figure 1, was obtained from the pump laser spectrum and the absorption probability spectrum, which was calculated from the absorption spectrum.

The pump−probe experiment on the bR sample was performed with a probe delay time of −400 to 800 fs. The change in absorbance caused by the pump pulse was probed as a function of the probe delay. The curve of the absorbance change versus delay is called the real-time (vibration) trace and the curve

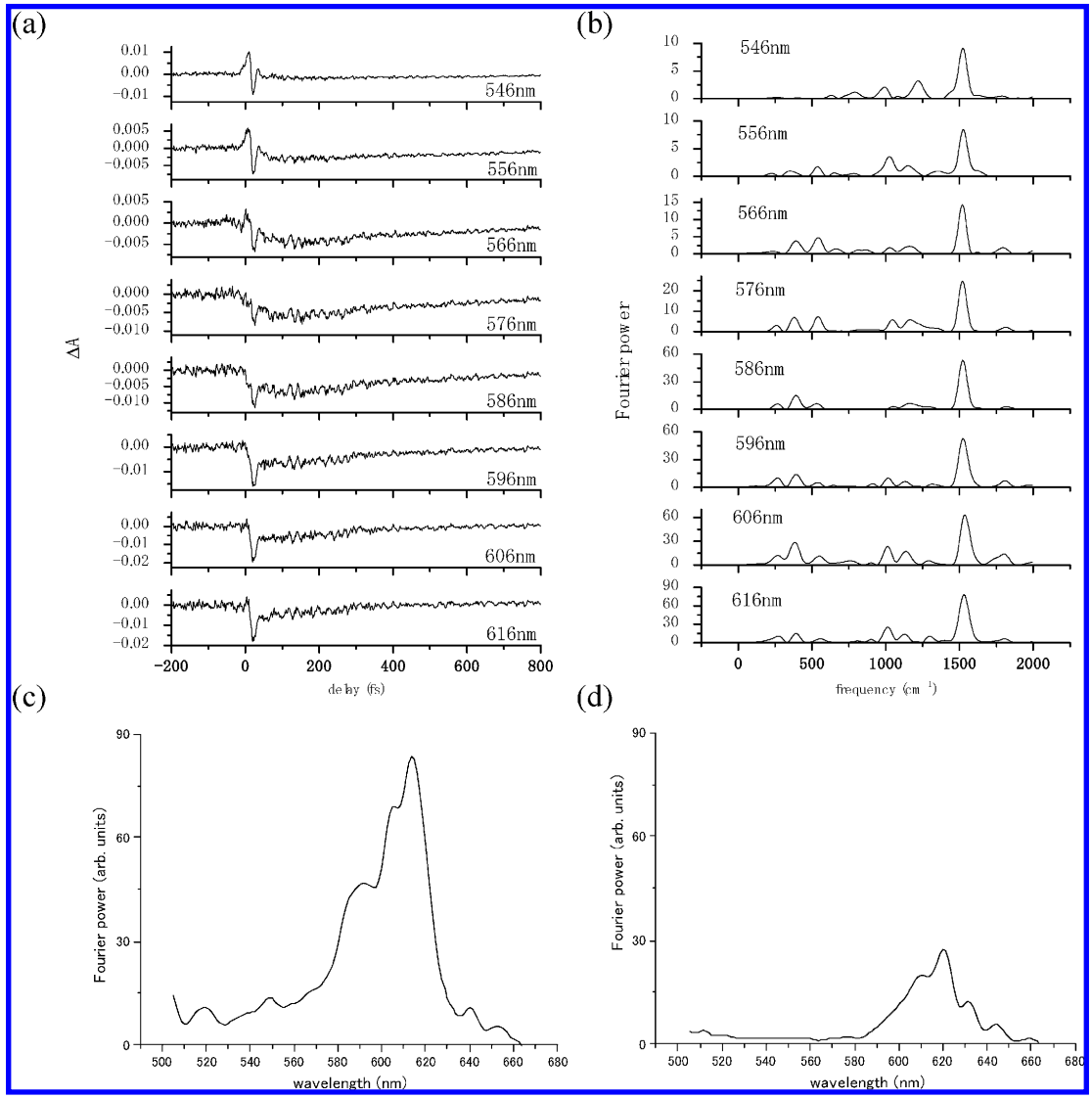

Figure 2. (a) Real-time traces and (b) Fourier power spectra of traces calculated from 50 to 800 fs at eight typical wavelengths. Fourier power spectra of the (c) 1527 and (d) 1008 cm^{-1} modes.

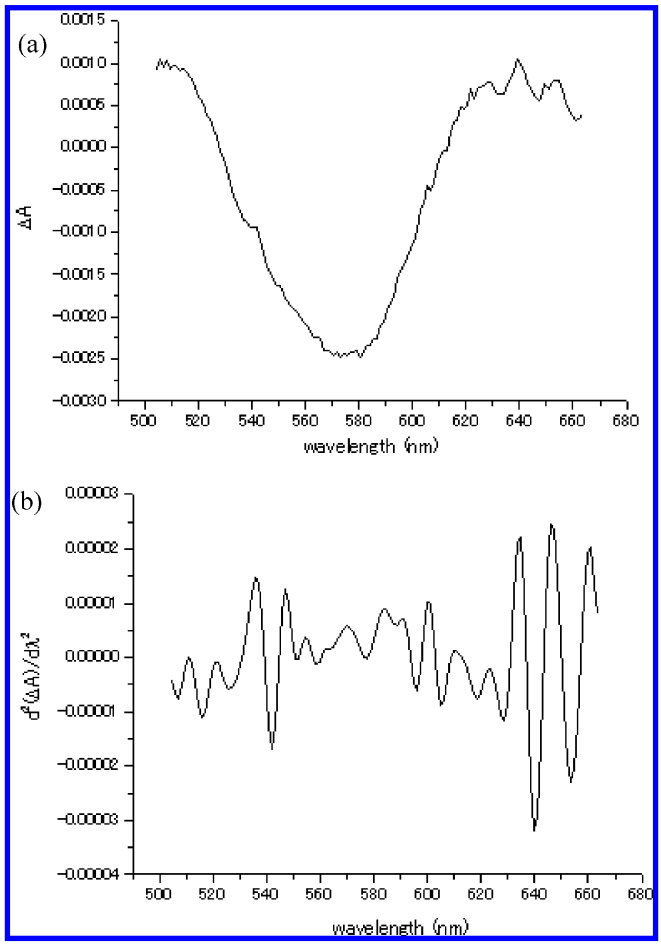

Figure 3. (a) Time-resolved spectrum of sample integrated from 400 to 800 fs and (b) its second derivative.

of the absorbance change versus probe wavelength is called the vibration real-time spectrum.

Panels a and b of Figure 2 present the real-time traces and Fourier power spectra of the traces, calculated from 50 to 800 fs, respectively, at eight typical wavelengths. The Fourier transform was performed from a time other than 0 fs, to eliminate any effect of interference between the probe pulse and the scattered pump pulse close to zero delay. Even though the pulse duration was sub-10 fs, the spatial coherence was very high and the multiply scattered pump pulse interfered with the probe pulse. Therefore, probe delays shorter than 50 fs had to be eliminated to prevent this effect of coherence. The power spectra in Figure 2b include two intense peaks at 1527 and 1008 cm^{-1}. Recently, time-resolved Raman spectra of bacteriorhodopsin were reported by the groups of Mathies and of Mizutani in 2009.[32,33] Figure 2b resembles Raman spectra of early delay time range shown in their reports. Therefore, Fourier power spectra shown in Figure 2b are thought to be mainly reflecting the J intermediate, which has an isomerized structure. Panels c and d of Figure 2 display the relative powers of the oscillations at 1527 and 1008 cm^{-1}, respectively, in the real-time traces measured at various wavelengths.

Figure 3a shows the time-resolved spectrum of the sample integrated over the range from 400 to 800 fs. It is referred to as the ΔA spectrum below. Previous study by Heller has theoretically predicted that fine structure on absorption spectrum reflects a time-correlation function, which is periodically modulated by wave packet motion on the potential energy surface.[34] The relation between optical

TABLE 1: Peak and Valley Frequencies in Fourier Power Spectra of 1527 and 1008 cm^{-1} Modes, in the ΔA Spectra, and in $d^2(\Delta A)/d\lambda^2$

1527 cm^{-1}		1008 cm^{-1}		ΔA		$d^2(\Delta A)/d\lambda^2$	
peak	valley	peak	valley	peak	valley	peak	valley
			15 180		15 140	15 166	
15 296		15 325		15 301			15 286
	15 444		15 533		15 456	15 451	
15 625		15 655					
	15 748		15 625	15 620			15 620
		15 841			15 791	15 755	
			15 904	15 893			15 884
					16 010	15 984	
				16 054			16 070
		16 129			16 151	16 135	
				16 185			16 212
16 293			16 326		16 304	16 291	
		16 393		16 348			16 366
	16 460				16 456	16 443	
16 528				16 501			16 526

absorption intensity $I(\omega)$ and time-correlation function of the transition dipole moment was obtained as follows:[35]

$$\int_{-\infty}^{\infty} \frac{I(\omega)}{\omega} = \sum_u \sum_v \rho_u \langle\langle \{iu|\mu(0)|fv\} \cdot \{fv|\mu(t)|iu\} \rangle_{ah} \rangle_{slv}$$
$$\equiv \langle\langle \mu_{if}(0) \cdot \mu_{if}(t) \rangle\rangle_0$$

where $\mu_{if}(0) = (i|\mu|f)$ and $\mu_{if}(t) = (i|\mu(t)|f)$. $|iu\}$ and $|fv\}$ denote the initial and final vibronic states. μ is the dipole moment operator written by

$$\mu = e \sum_a r_a$$

where a is the ath electron of a solute molecule. ρ_u is the state density of the iu state. Kakitani et al. has applied this method for the study of stationary absorption spectrum of bR.[36]

As is seen in Figure 3a, the time-resolved absorption change ΔA observed in this work shows fine structure of ~150 cm^{-1} period in the spectral region where ΔA has a positive value dominated by the effect of induced absorption. The period of 150 cm^{-1} agrees with the reported values of torsion period around C_{12}=C_{13}.[29,37,38] Therefore, the observed fine structure is thought to be reflecting anharmonicity of the torsion mode in the higher excited state, which is the final state of the induced absorption process. The spectral features are thus observed by freezing the wavepacket motion in the excited stae revealing the large displacement along the potential curve corresponding to the torsion not only in the lowest excited state but also in the higher excited state, which is located higher than the lowest excited state by 16 000 cm^{-1}. The resilt is very reasonable becasue the instability of the lowest excited state to trigger the ultrafast torsion relevant to the photoisomerization is due to the change of the bond order and steric hindrance of the methyl group attached to C_{11}. To go into deeper discussion, calculation of the second derivative of the ΔA spectrum was performed. Peaks and valleys in the second derivative of the spectrum correspond to the hidden valleys and peaks in the ΔA (we call it zeroth derivative) spectrum. Hence, the second derivative of the ΔA spectrum in Figure 3b has a fine structure that has various peaks and valleys. We confirmed that the spectral

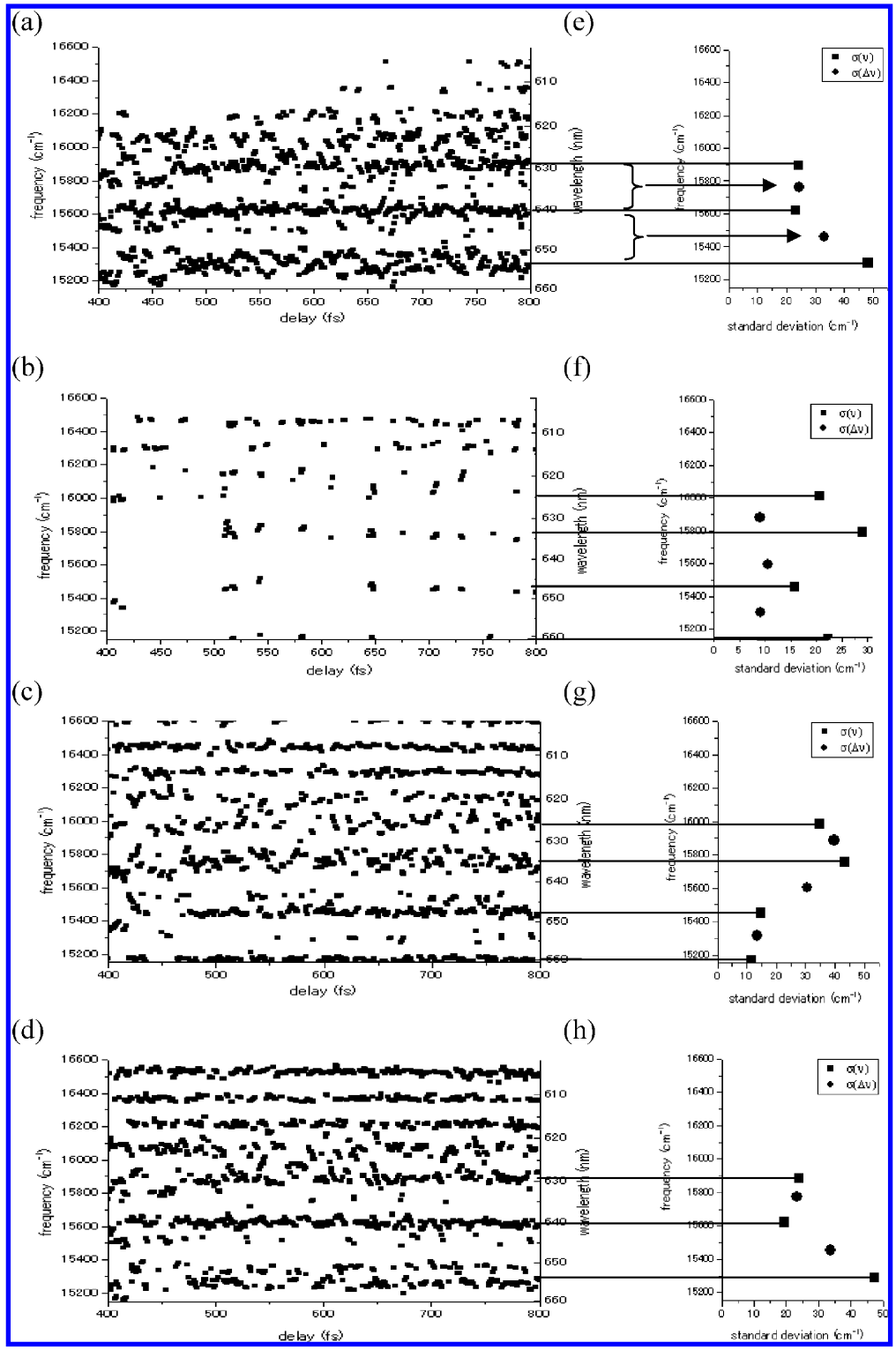

Figure 4. Dependence of (a) peak and (b) valley frequencies in ΔA spectra on delay. (c, d) Dependence of $d^2(\Delta A)/d\lambda^2$ thereon. At delays from 400 to 800 fs, standard deviation of peak [valley] frequencies ($\sigma(\nu)$; filled circle) and that of difference between frequencies of neighboring peaks [valleys] ($\sigma(\Delta\nu)$; filled square) were calculated for (e) [(f)] ΔA spectra and (g) [(h)] for $d^2(\Delta A)/d\lambda^2$.

structure is reproducible in all four different scans of data. The structure that is evident in the relative powers of the oscillations at 1527 and 1008 cm^{-1} (see Figure 2c,d) has peaks or valleys at close to the same photon energies as the ΔA spectrum and its second derivative. Table 1 presents the frequencies of the peaks and valleys in the Fourier power spectra, the ΔA spectrum, and its second derivative.

The ΔA signal reflects the modulation of electronic transition probability by wave packet motion on a potential energy surface. When the time-resolution of the measurement is much better than the period of wave packet motion associated with molecular vibrations of several tens of femtoseconds, the observed ΔA spectrum at each delay step reflects the spectral structure of electronic states with vibration modes. As was reported in our previous work,[25] the dynamics of bR is dominated by the J intermediate in the time region from 400 to 800 fs and the spectral region from 610 to 660 nm where the peaks and valleys were observed above in the time-resolved ΔA spectrum and

Fourier power spectra. Since the time-resolution of this work is better than 10 fs, the wave packet on the potential energy surface can be assumed to be motionless at a localized location on the surface corresponding to each probe delay in the time-resolved measurements. Therefore, the fine structures on the time-resolved ΔA spectra are thought to reflect the vibrational levels of the J intermediate, which was observed by freezing the position of the wave packet on the electronic state.

The distances between neighboring peaks or valleys are 153 ± 12 or 309 ± 27 cm^{-1}, respectively. Accordingly, peaks (valleys) correspond to the vibrational progression in the time-resolved spectrum that is associated with the excited state absorption (stimulated emission). Valley signals, associated with bleaching that is induced by the ground-state depletion, are thought to be negligible, because of the absence of sufficiently intense fluorescence at this low probe frequency (long wavelength).

Even though the peak (valley) positions may not be very precise, the frequency separations are almost the same, indicating that they still can be considered to represent the vibrational progression, which is sensitively revealed by the Fourier power spectrum. The frequency separations among these peaks and valleys are independent of the delay, indicating that the spectral shape of these valleys and peaks does not arise from spectral interference between the scattered pump and the probe. The spectral spacings of 153 and 309 cm^{-1} may be assigned to the fundamental and double frequencies of the twisting motion associated with photoisomerization that had an observed period of around 200 fs.[29,37,38]

Panels a and b of Figure 4 present the peak frequencies and valley frequencies, respectively, of ΔA spectra over a range of delays in steps of 1 fs. Panels c and d of Figure 4 show those of the second derivatives of the ΔA spectra. The standard deviations of the peak (valley) frequencies and of the frequency difference between the frequencies of the neighboring peaks (valleys) were calculated by using the data in panels a−d of Figure 4, and displayed in panels e−h of Figure 4, respectively. The range of delays used to calculate the standard derivation was from 400 to 800 fs, to avoid any interference between the probe pulse and the scattered pump pulse. A mean frequency of neighboring peaks was used as the abscissa in the plot of the standard deviation of the difference between frequencies. If the neighboring peaks (valleys) move independently of each other, then the standard deviation of difference between the frequencies of the neighboring peaks (valleys) should be $\sqrt{2}$ times that of the peak (valley) frequencies themselves as expected from the Gaussian random statistics. However, the ratio of the former to the latter was in fact observed to be 0.90 ± 0.24, which is much smaller than $\sqrt{2}$. Therefore, neighboring peaks (valleys) move in a synchronized way, verifying that vibrational progression appears as the spectral structure, which is revealed by data.

4. Conclusions

In conclusion, for the first time, the vibrational progression that is hidden in a featureless spectrum of induced absorption and stimulated emission is found by using the Fourier power spectrum of molecular vibrational modes, because of the localization of the wave packet along the potential multimode hyper surfaces. The transition energy of the induced absorption or stimulated emission corresponds to a localized point (space) on the hyper surface, which the wave packets visit with fixed phases.

Acknowledgment. This work was partially supported by the 21st Century COE program on "Coherent Optical Science", by a grant to A.Y. from the National Science Council of the Republic of China, Taiwan (NSC 98-2112-M-009-001-MY3), and by a grant from the Ministry of Education (MOE) of the Republic of China, Taiwan, under the ATU Program at National Chiao-Tung University. Part of this work was conducted as part of a joint research project on laser engineering, Osaka University, under contract B1-27. Ted Knoy is appreciated for his editorial assistance.

References and Notes

(1) Shreve, A. P.; Mathies, R. A. *J. Phys. Chem.* **1995**, *99*, 7285–7299.
(2) Gonzáles-Luque, R.; Garavelli, M.; Bernardi, F.; Merchan, M.; Robb, M. A.; Olivucci, M. *Proc. Natl. Acad. Sci. U.S.A.* **2000**, *97*, 9379–9384.
(3) Humphrey, W.; Lu, H.; Logonov, I.; Werner, H. J.; Schulten, K. *Biophys. J.* **1998**, *75*, 1689–1699.
(4) Schenki, S.; van Mourik, F.; van der Zwan, G.; Haacke, S.; Chergui, M. *Science* **2005**, *309*, 917–920.
(5) Herbst, J.; Heyne, K.; Diller, R. *Science* **2002**, *297*, 822–825.
(6) Haran, G.; Wynne, K.; Xie, A.-H.; He, Q.; Chance, M.; Hochstrasser, R. M. *Chem. Phys. Lett.* **1996**, *261*, 389–395.
(7) Gai, F.; Hasson, K. C.; McDonald, J. C.; Anfinrud, P. A. *Science* **1998**, *279*, 1886–1891.
(8) Zhong, Q.; Ruhman, S.; Ottolenghi, M. J. *J. Am. Chem. Soc.* **1996**, *118*, 12828–12829.
(9) Song, L.; El-Sayed, M. A. *J. Am. Chem. Soc.* **1998**, *120*, 8889–8890.
(10) Du, M.; Fleming, G. R. *Biophys. Chem.* **1993**, *48*, 101–111.
(11) Roy, S.; Singh, C. P.; Reddy, K. P. J. *Curr. Sci.* **2002**, *83*, 623–626.
(12) Kahan, A.; Nahmias, O.; Friedman, N.; Sheves, M.; Ruhman, S. *J. Am. Chem. Soc.* **2007**, *129*, 537–546.
(13) Hou, B.-X.; Friedman, N.; Ottolenghi, M.; Sheves, M.; Ruhman, S. *Chem. Phys. Lett.* **2003**, *381*, 549–555.
(14) Terentis, A. C.; Zhou, Y.; Atkinson, G. H.; Ujj, L. *J. Phys. Chem. A* **2003**, *107*, 10787–10797.
(15) Olivucci, M.; Lami, A.; Santoro, F. *Angew. Chem., Int. Ed.* **2005**, *44*, 5118–5121.
(16) Hayashi, S.; Tajkhorshid, E.; Schulten, K. *Biophys. J.* **2003**, *85*, 1440–1449.
(17) Rose, T. S.; Rosker, M. J.; Zewail, A. H. *J. Chem. Phys.* **1988**, *88*, 6672–6673.
(18) Polanyi, J. C.; Zewail, A. H. *Acc. Chem. Res.* **1995**, *28*, 119–132.
(19) Prokhorenko, V. I.; Nagy, A. M.; Waschuk, S. A.; Brown, L. S.; Birge, R. R.; Miller, R. J. D. *Science* **2006**, *313*, 1257–1261.
(20) Srinivasan, R.; Feenstra, J. S.; Park, S. T.; Xu, S.; Zewail, A. H. *Science* **2005**, *307*, 558–563.
(21) Schotte, F.; Soman, J.; Olson, J. S.; Wulff, M.; Anfinrud, P. A. *J. Struct. Biol.* **2004**, *147*, 235–246.
(22) Kobayashi, T.; Saito, T.; Ohtani, H. *Nature* **2001**, *414*, 531–534.
(23) McCamant, D. W.; Kukura, P.; Mathies, R. A. *Appl. Spectrosc.* **2003**, *57*, 1317–1323.
(24) Kahan, A.; Nahmias, O.; Friedman, N.; Sheves, M.; Ruhman, S. *J. Am. Chem. Soc.* **2007**, *129*, 537–546.
(25) Yabushita, A.; Kobayashi, T. *Biophys. J.* **2009**, *96*, 1–15.
(26) Shirakawa, A.; Sakane, I.; Kobayashi, T. *Opt. Lett.* **1998**, *23*, 1292–1295.
(27) Shirakawa, A.; Sakane, I.; Takasaka, M.; Kobayashi, T. *Appl. Phys. Lett.* **1999**, *74*, 2268–2270.
(28) Baltuska, A.; Fuji, T.; Kobayashi, T. *Opt. Lett.* **2002**, *27*, 306–308.
(29) Kobayashi, T.; Saito, T.; Ohtani, H. *Nature* **2001**, *414*, 531–534.
(30) Kobayashi, T.; Shirakawa, A.; Matsuzawa, H.; Nakanishi, H. *Chem. Phys. Lett.* **2000**, *321*, 385–393.
(31) Ishii, N.; Tokunaga, E.; Adachi, S.; Kimura, T.; Matsuda, H.; Kobayashi, T. *Phys. Rev. A* **2004**, *70*, 023811.
(32) Shim, S.; Dasgupta, J.; Mathies, R. A. *J. Am. Chem. Soc.* **2009**, *131*, 7592–7597.
(33) Mizuno, M.; Shibata, M.; Yamada, J.; Kandori, H.; Mizutani, Y. *J. Phys. Chem. B* **2009**, *113*, 12121–12128.
(34) Heller, H. J. *J. Chem. Phys.* **1978**, *68*, 3891–3896.
(35) Kakitani, T. *J. Phys. Soc. Jpn.* **1986**, *55*, 993–1010.
(36) Akiyama, R; Kakitani, T; Imamoto, Y.; Shichida, Y.; Hatano, Y. *J. Phys. Chem.* **1995**, *99*, 7147–7153.
(37) Chen, X.; Batista, V. S. *J. Photochem. Photobiol., A* **2007**, *190*, 274–282.
(38) Mayers, A. B.; Harris, R. A.; Mathies, R. A. *J. Chem. Phys.* **1983**, *79*, 603–613.

JP9090014